# Evaluation of a lightweigth UAS-prototype for hyperspectral imaging.

K. Nackaerts[a], B. Delauré[a], J. Everaerts[a],B. Michiels[a], C. Holmlund[b], J. Mäkynen[b], H. Saari[b]

a Flemish Institute for Technological Research - VITO, Boeretang 200, BE-2400 Mol, Belgium
b Technical Research Centre of Finland - VTT, P.O. Box 1000, FI-02044 VTT, Finland

**ICWG I/V**

**KEY WORDS: hyperspectral imaging, Fabry-Perot, rotorcraft, mapping, light-weight UAS**

## ABSTRACT:

Recent developments in the area of miniaturisation have boosted the development of a wide range of Unmanned Aerial Systems (UAS). In terms of hyperspectral imaging, no appropriate sensors are available for light weight UAS. Available sensors are in general too heavy, produce an overload on data, and are mainly 1D line sensors. Given the attitude instability of a light weight UAV in combination with inferior miniaturized attitude sensors, accurate image reconstruction becomes an exceptional challenge for such line sensors mounted on a UAS.

The first trials with a novel UAS equipped with an hyperspectral frame imager are presented. The imager was integrated and operated on a six-rotor rotorcraft type UAV of VITO, the Flemisch Institute for Technological Research. This system provides an answer to the above mentioned issues: two dimensional imaging, low weight and with user definable (application specific) spectral sensitivity. The hyperspectral imager was developed by VTT Technical Research Centre of Finland and is based on the Piezo actuated Fabry-Perot Interferometer to enable recording of 2D spatial images at the selected wavelength bands simultaneously and to reduce the size of the hyperspectral spectrometer to be compatible with light weight UAV platforms. The prototype is capable of recording 2D images within the range of 400 – 1100 nm at a spectral resolution of 5 – 10 nm @ FWHM. The full sensor system (sensor, storage, battery and triggering) weighted less than 500 grams. The results and key issues for improvement for different aspects of the UAS will be presented during the symposium.

## 1. INTRODUCTION

One of the main challenges for small low altitude Unmanned Aerial Systems hereby is the development, testing and calibration of suitable sensors that provide information of interest to the end user. Weight and power consumption are the most limiting factor and put new constraints on sensor development. The potential of available technology is surfacing on a regular basis. Aerial imaging is feasible today by means of standard digital consumer camera's. Grenzdörffer et al. (2008) describes the potential of low cost UAVs equipped with such cameras for photogrammetric applications. Eisenbeiss et al. (2008) and Lambers et al. (2007) complemented photogrammetry based on a standard DSLR camera successfully. This work has been continued by Eisenbeiss et al. (2008) and tested to create an accurate 3D reconstruction of an historical building illustrating the technology's full potential for very high resolution applications. MacArthur et al. (2006) use an industrial mini stereo RGB vision system to map citrus yields. The results were promising, but a higher spectral resolution was necessary.

When adding narrow bandwidth optical filters to a digital camera, multispectral imaging becomes available, allowing to extract specific surface properties of interest. This can be performed by using consumer or industrial cameras as used by Chao et al. (2008) in a research project to study the feasibility of a UVS for real-time water management and irrigation control. Nebiker et al. (2008) demonstrate the use of industrial smart cameras for multispectral imaging. A more dedicated system –a combination of multiple CMOS cameras in a fixed frame setup with exchangeable filters- was used by Suarez et al. (2009) for crop monitoring. This work demonstrate that results obtained with a low-cost UAS for agricultural applications yielded comparable estimations than those obtained by tradi-

tional manned airborne systems. Zarco-Tejada et al. (2009) proved that even more complex fluorescence measurements are possible by means of a small helicopter UVS and multi-spectral camera.

Because of weight issues of the above mentioned multispectral solutions and the potential information content in hyperspectral images, manufacturers of hyperspectral imagers have also been working on the miniaturisation of their systems to allow integration in industrial environments and the UVS market. Ramanathan (2006) and describes the potential of the use of small hyperspectral imaging and non-imaging sensors in a UAS. Esposito et al. (2007) describe the development and first test flights of a fixed wing UVS, equipped with a 170 channel spectral imager from Specim (http://www.specim.fi/). Reymer et al. (2008) use a hyperspectral line scanner mounted below a helicopter system to study tidal flats. However, the hyperspectral imagers mentioned above are still relatively heavy (> 2kg), large, not easily integrable (require extra datalogger) and line scanners. The main drawback of a line scanner on a small UAS is the difficulty to reconstruct a 2D image because of the inherent instability of such a UAS.

Next to the high spatial resolution and flexibility regarding data acquisition time (no fixed overpass times, less sensitive to weather conditions), the high temporal resolution is an important discriminator of UAS. Agriculture crops can be studied at relevant revisit times. Planer-Friedrich et al. (2008) for example used a balloon with a standard digital consumer camera to monitor changes in Yellowstone national park. An important aspect of time series analysis is the required sub-pixel accurate georegistration of multitemporal imagery.

In this paper a novel approach is presented whereby a lightweight prototype Fabry-Perot Interferometer spectral imager -developed by VTT- is interfaced on a light weight UAS of VITO. The system has the ability to record 2D spectral images at user selected spectral bands and this at a total payload weight below 350 grams. This includes data capture and storage capabilities. Because of the compact dimensions, the mechanical interface requirements are compatible with most light weight UAS.

## 2. HYPERSPECTRAL UAS

### 2.1 Hyperspectral imager application requirements

Objectives of the first trials of hyperspectral imager were agreed by the research teams of VITO and VTT. The agreed objectives were

- To operate the hyperspectral imager on the Draganfly X6 UAS helicopter and on a telescope mast
- To evaluate the geometric and radiometric performance of the VTT hyperspectral instrument from the X6 UAV by using reference targets
- To evaluate the VTT hyperspectral imager for vegetation classification purposes.
- To evaluate potential for stress detection in vegetation.

The spectral bands selected for the first trials were 550, 650, 710 and 800 nm and the required spectra resolution was < 10 nm @ FWHM.

### 2.2 The Platform

The platform is an X6 hexacopter from Draganfly (http://www.draganfly.com) and is illustrated in Figure 1.

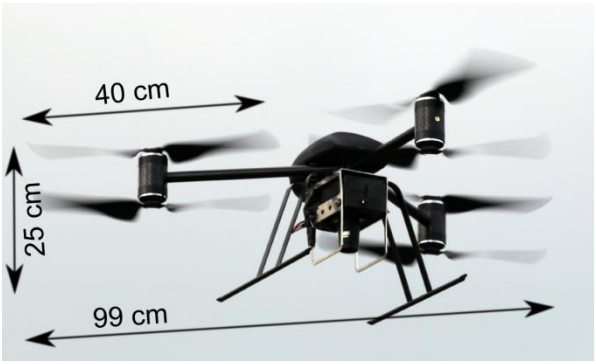


Figure 1. Draganfly X6 UAS Helicopter

A specific interface was developed to allow the use of the build in camera control unit of the X6 patform. For this, a microcontrollerboard was programmed to generate a specific trigger to the hyperspectral imager from an input from this unit. Exterior orientation was recorded on the datalogger of the X6, together with the camera trigger actions.

### 2.3 Overview of Staring Fabry-Perot Interferometer (FPI) Hyperspectral Imager Concept

**Error! Reference source not found.**The hyperspectral imager records simultaneously a 2D image of the scenery at three narrow wavelength bands determined by the selected three orders of the Fabry-Perot Interferometer which depend on the air gap between the mirrors of the Fabry-Perot Cavity. The concept is explained in the plots of **Error! Reference source not found.**. In the upper part there are plots of spectral transmission of the FPI for orders 2, 3 and 4 with an air gap of 0.85 µm. In this concept the light from the object is collimated by the front optics and the collimated beam is directed to the FPI cavity and order sorting filter. This combination passes only one narrow wavelength band determined by the air gap value and the selected FPI order filter. The focusing optics focuses the light transmitted through the FPI to an object image at one narrow wavelength band. It is obvious that the light beam through the FPI is not totally collimated and that this will have an effect on the spectral resolution of the instrument. When low orders of the FPI (1 - 4) are used the spectral resolution is not dominated by the collimation level of the optical beam as far as the incident angle is below around 5 degrees. The novel concept utiliz-

ing multiple orders of Fabry-Perot Interferometer is illustrated by the plotted transmission of the FPI and the quantum efficiency of the RGB imager sensor and of a combined spectral response of FPI and Image sensor.

### 2.4 Instrument performance and interface requirements

The instrument and interface requirements were derived based on the selected applications and the available UAS platform. The major requirements are listed in Table 1.

| Parameter | Requirement |
|---|---|
| Spectral range | 500 – 900 nm |
| Spectral resolution | < 10 nm @ FWHM |
| Spectral sampling step size | < 1 nm |
| Stability of the wavelength scale | < 0.1 nm |
| Time required to change the wavelength band | < 2 ms |
| F-number of the optics | < 5.6 |
| Angular field of view of the optics | > 20° in vertical dir.<br>> 30° in horiz. dir. |
| Image size | Wide VGA 480 x 750 pixels |
| Dynamic range | 10 bits |
| Weight of the whole instrument | < 350 g |
| Image Memory capacity | > 2 Gbyte |
| Trigger mode | TTL pulse from Autopilot |

Table 1: Goal instrument requirements for the FPI and multispectral image sensor based hyperspectral imager

### 2.5 Optics design

The optics design of a staring spectral imager with a wide VGA resolution can be based on a standard video objective. The operational spectral bandwidth is defined by the low pass filter with cutoff at 900 nm (Edmund Optics Techspec short pass filter M47-820) and a high pass filter with 500 nm cutoff (Edmund Optics High Performance high pass filter M62-976). The used video objective is Fujinon YF8A-2 which has a 8 mm focal length and manual focus and iris adjustment capability. The F-number was fixed to 5.6 +- 0.2 for all tests. The ground pixel size is 7.5 cm at 100 m altitude and FOV is 20.4 $^{o}$ in flight and 31.4$^{o}$ across the flight direction.

### 2.6 Control electronics design

A description of the electronics of the hyperspectral imager platform is shown by the block diagram of Figure 2Figure . The spectrometer control board can control either one or two Fabry-Perot interferometer modules simultaneously. The spectrometer control board also controls the data flows from the image sensor to flash memory and from the memory to the computer through a USB2-interface. The system includes two light sensors which can be used to monitor spectral radiance of the scenery and the solar spectral irradiance. The parts of hyperspectral imager and an integrated module are presented in Figure 3.

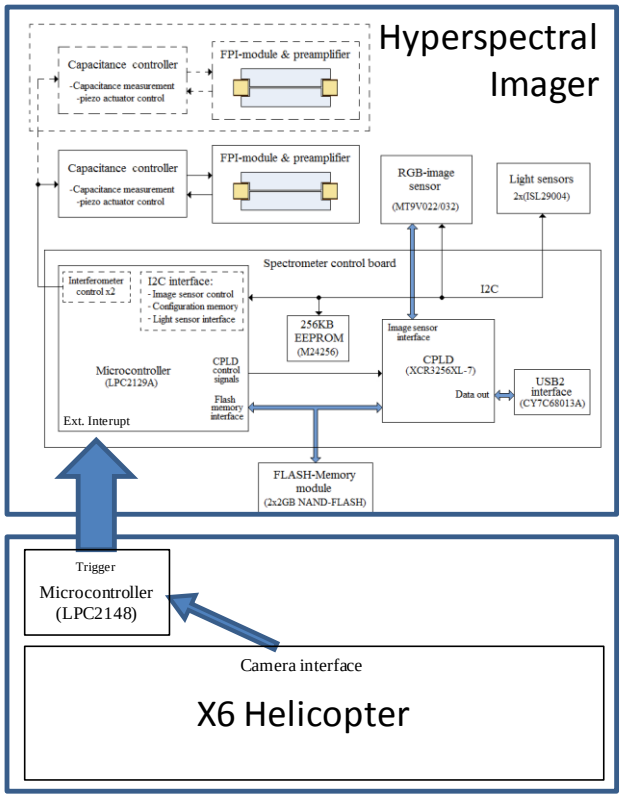


Figure 2: A block diagram of the control electronics of the Staring FPI Hyperspectral Imager.


Figure 3: The parts of Staring FPI Hyperspectral Imager and an integrated equipment. The envelope is 100 mm x 70 mm x 53 mm, The objective tube extends out of the main structure by 35 mm.

## 3. STARING FPI HYPERSPECTRAL IMAGER TEST FLIGHTS WITH DRAGANFLY X6

Due to flight restrictions active in Belgium, test flights with the VITO six-rotor rotorcraft type Draganfly X6 were performed on 28.-30.9.2009 at Meerhout (Belgium) on an small airfield preserved for model airplanes. The main goal was to testfly the fully integrated system and acquire hyperspectral images.

The VTT Staring FPI Hyperspectral Imager integrated on X6 is shown in Figure 4. Different test targets were used (see Figure 5) to assess the radiometric and geometrical imaging performance of the imager. The first trials were performed using the four selected wavelength bands (550, 650, 710&800 nm) taking

the exposures at these bands in sequence. The exposure times of 2, 5, 10 20 and 40 ms were used.

The 40 ms image data was mostly saturated and 2 ms was too short exposure time at the "half cloudy weather" during tests. The image quality in tests was naturally dependent on the exposure time, stability of the plane and imaging optics. The data of test flights has so far been processed by converting a raw data RGB image to images at 3 wavelength bands. The generation of a mosaic image at selected wavelength has not yet been performed. A video clip of Hyperspectral imager data from the X6 test flight has been generated. The raw image data shows that the system can provide 2D image data that can be used for an accurate image reconstruction.

Figure 4: VTT Staring FPI Hyperspectral Imager integrated on VITO six-rotor rotorcraft type Draganfly X6

Figure 5: Test targets used in the evaluation of the hyperspectral imager performance.

## 4. DATA ANALYSIS

### 4.1 Image processing

A major issue with this type of relative low resolution imagery data, acquired from a small and inherently unstable UAS is image coregistration. This is especially true for this type of imager whereby multiple wavelengths are images sequentially over time. During the testflight, a range between 600 and 1130 nm was imaged. Because the mirrors of the Fabry-Perot need time to switch, this results in image displacements and distortions. These are caused by wind and (auto) piloting effects of the UAS platform. Figure 6 illustrates this:

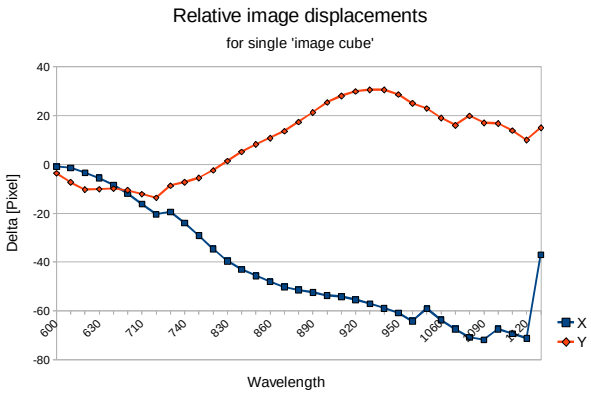


Figure 6: Relative displacement of sequential image frames calculated from optical flow velocity vectors.

To allow efficient use of this novel type of data such as spectral signature extraction and in the future time series analysis, accurate and flexible image coregistration is of utmost importance. Direct image registration is difficult: the exterior orientation estimates –position and attitude- from this small UAS are of low quality and cannot be used directly. Moreover, issues with time-stamping the images are present adding uncertainties. Therefore, a first approach tested is based on traditional image processing techniques whereby a perspective transformation matrix is estimated for each image frame with respect to a fixed reference image of the study area. The reference image is build from an initial flight with the UAS and a commercial RGB camera. A single image as taken from the UAS is illustrated in Figure 7:

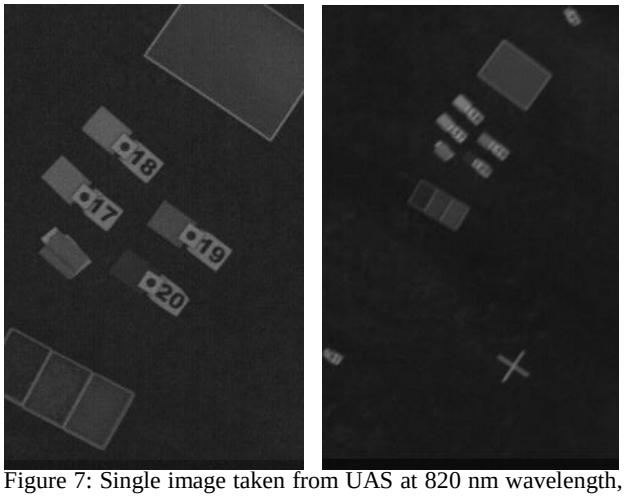


Figure 7: Single image taken from UAS at 820 nm wavelength, from different flying heights.

The following workflow was implemented and tested to register each image frame with respect to the reference:

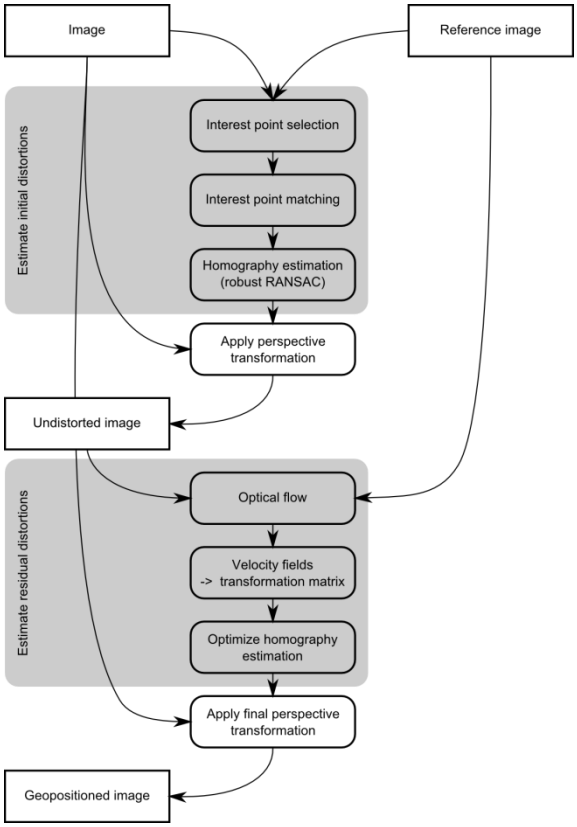


Figure 8: Robust image co-registration workflow

Finally when co-registration is successfull, spectral profiles are reconstructed for each spectral target of interest and further analysed. Because of the explorative character of this first experiment and the fact that no absolute calibration of the system was performed at the time of the experiment all measures analysed are relative measures. First, spectral variability for single feature types (spectral target) is analysed. Second, spectral signatures are compared for different targets and their reference measurements with a calibrated field spectroradiometer (ASD Fieldspec Pro). Inter-comparison of spectral signatures is done based on the spectral angular mapper algorithm. The Spectral Angle Mapper (SAM; Kruse et al. 1996) is a physically-based algorithm that calculates the similarity between two spectra, expressed as the angle between two vectors. Each vector corresponds hereby to a single spectral signature described by reflectance or digital numbers values for each wavelength measured in an n-dimensional (number of bands) space. This measure has been described as being relatively robust with respect to illumination and albedo effects.

## 5. RESULTS

The results provide a first insight in the potential of this noval hyperspectral imaging system when used on a small lightweight UAS and will be presented during the conference.

## 6. CONCLUSIONS

A staring hyperspectral payload with total system mass of 350 g including image memory, batteries has been presented. The operational wavelength range is 500 – 900 nm and the spectral resolution < 10 nm @ FWHM. The exposure times of 5 - 10 ms proved to be adequate at the “half cloudy weather” during tests. The ground pixel size is 7.5 cm at 100 m altitude and FOV is 20.4 $^{o}$ in flight and 31.4$^{o}$ across the flight direction. The imager is compatible with light weight UAS (total weight 1 – 2 kg) interface requirements. It was shown that the imager can operate on a six-rotor rotorcraft UAS (Draganfly X6). The spectral imaging at the user defined wavelength bands was demonstrated in vegetation applications. Further data analysis work is required to evaluate the accuracy at which the image reconstruction can be performed for the selected wavelength band images. The spectral data cube image reconstruction must also be studied in more detail. The software to generate spectral images at three narrow wavelength band from the raw RGB data provides radiometrically calibrated data for most raw images but further development is still needed to remove the remaining false results in the conversion of the raw data images to images at 3 wavelengths. The framing hyperspectral imager requires special software to calculate the mosaic hyperspectral data cube from the separate spectral overlapping images.

The major items that would improve the system performance are higher sensitivity and dynamic range of the RGB image sensor, wider operational wavelength range, larger Field of View and higher spatial resolution to simplify image registration. With respect to interfacing, a specific interface for timestamping should be added.

All these items have been analyzed and in the next prototype most of them will be improved. The major improvement is achieved via changing the image sensor to 5 Mpix CMOS Image sensor MT9P031 from Aptina. The optics can be designed to provide > 45 degree FOV. The wider operational wavelength range can be achieved by using two RGB image sensors.

Successfull applications with this novel UAS are only guaranteed when automated data processing is available. A first step in the image analysis will always be accurate image geo-rectification. Further research will be performed on this topic.

## 7. REFERENCES

Aptina Ltd. http://www.aptina.com/products/image_sensors/mt9p031i12stc/#overview

Chao, H., Baumann, M., Jensen, A. M., Chen, Y., Cao, Y., Ren, W., and McKee, M. Band-reconfigurable multi-uav-based cooperative remote sensing for real-time water management and distributed irrigation control. Proceedings of the IFAC World Congress. Seoul, South Korea (2008).

Draganfly Innovations Inc., http://www.draganfly.com/uav-helicopter/draganflyer-x6/specifications/

Eisenbeiss, H., Sauerbier, M., and Pueschel, H. Kombinierte auswertung von terrestrischen und uav-bildern für die 3d-modellierung des schlosses landenberg. Geomatik Schweiz, 470–473 (2008).

Esposito, F., Rufino, C., Moccia, A., Donnarumma P., Esposito, M., Magliulo, V., "An Integrated Electro-Optical Payload System for Forest Fires Monitoring from Airborne Platform", in Proc. IEEE Aerosp. Conf., pp. 1–13 (2007).

Grenzdörffer, G., Engel, A. and Teichert, B. The Photogrammetric Potential of Low-Cost UAVS in Forestry and Agriculture, The International Archives of the Photogrammetry, Remote Sensing and Spatial Information Sciences, XXXVII. Part B1, ISPRS Congress, Beijing, China, 1207-1213 (2008).

Herwitz, S., Johnson, L., Dunagan, S., Higgins, R., Sullivan, D., Zheng, J., Lobitz, B., Leung, J., Gallmeyer, B. Aoyagi, M. Slye, R.and Brass, J., "Coffee field ripeness detection using high resolution imaging systems of a solar-powered UAV," roc. of 30th Int'l Symp. Rem. Sens. Environ. (2003a).

Johnson, L.F., Herwitza, S., Dunagana, S., Lobitza, B., Sullivan, D., Slyea, R.,"Collection of Ultra High Spatial and Spectral Resolution Image Data over California Vineyards with a Small UAV", Proc. of 30th Int'l Symp. Rem. Sens. Environ. (2003a).

Kruse, F.A., J.W. Boardman, A.B. Lefkoff, K.B., Heidebrecht, A.T. Shapiro, P.J. Barloon, and A.F.H. Goetz. The Spectral Image Processing System (SIPS): Interactive visualization and analysis of imaging spectrometer data. Remote Sensing of Environment 44: 145-163 (1993).

Lambers, K., Eisenbeiss, H., Sauerbier, M., Kupferschmidt, D., Gaisecker, T., Sotoodeh, S., and Hanusch, T. Combining photogrammetry and laser scanning for the recording and modelling of the late intermediate period site of pinchango alto, palpa, peru. Journal of Archaeological Science, 34, 1702–1712 (2007).

MacArthur, D. K., MacArthur, E. Z., Schueller, J. K., Lee, W. S., Crane, C. D., and Parsons, L. R. Remotely-piloted helicopter citrus yield map estimation. Proceedings of ASABE Annual International Meeting. Portland, Oregon, US (2006).

Nebiker, S., Annen, A., Scherrer, D., and Oesch, D. A light-weight multispectral sensor for micro uav – opportunities for very high resolution airborne remote sensing. Paper presented at 21st Congress of the International Society for Photogrammetry and Remote Sensing (ISPRS), Beijing, China (2008).

Ramanathan, V. Western pacific autonomous uav campaign, aerosol-dust-cloud interactions and climate effects DOE, NASA, NOAA and NSF (2006).

Reymer, A., Peyaud, A., and van 't Hof, J. Low altitude remote sensing with UAS. in: Unmanned Aircraft Systems: The Global Perspective, 120-121 (2008).

Planer-Friedrich, B., Becker, J., Brimer, B., and Merkel, B. J. Low-cost aerial photography for high-resolution mapping of hydrothermal areas in yellowstone national park. International Journal of Remote Sensing, 29(6), 1781–1794 (2008).

Saari, H., Aallos, V., Akujärvi, A., Antila, T., Holmlund C., Kantojärvi, U., Mäkynen, J. and Ollila J., "Novel Miniaturized Hyperspectral Sensor for UAV and Space Applications", Proc. SPIE 7474 (2009).

Specim Ltd, "ImSpector imaging spectrographs", product brochure (2009).

Headwall Photonics Ltd, "MicroHyperspec® imaging spectrographs", product brochure (2009).

Sripada, R.P., D.C. Farrer, R. Weisz, R.W. Heiniger, and J.G. White. Aerial color infrared photography to optimize in-season nitrogen fertilizer recommendations in winter wheat, Agron. J., 99:1424-1435 (2007).

Suárez, L., Zarco-Tejada, P. J., Berni, J. A. J., González-Dugo, V., and Fereres, E. Modelling pri for water stress detection using radiative transfer models. Remote Sensing of Environment, 113(4), 730–744 (2009).

Zarco-Tejada, P. J., Berni, J. A. J., Suárez, L., Sepulcre-Cantó, G., Morales, F., and Miller, J. R. Imaging chlorophyll fluorescence with an airborne narrow-band multispectral camera for vegetation stress detection. Remote Sensing of Environment (2009).